

Mathematical Approach for Verifying Buckling in Steel Plates.

<http://www.doi.org/10.62341/licase2078>

Abdelmoutalib BENFRID

(ORCID: 0009-0007-8171-1654)
LSMAGCTP/ FT/ UDL-SBA, Algeria
ATRST, Algeria
benfridabdelmoutalib2050@gmail.com
+213-696939173

Mohamed Bachir Bouiadjra

(ORCID: 0009-0008-4814-6187)
LSMAGCTP/ FT/ UDL-SBA, Algeria
ATRST, Algeria
Email: mohamedbachirbouiadjra@gmail.com
+213-661200447

Abstract:

A mathematical study was conducted to investigate the buckling of isotropic steel plates using instability theories. The First-Order Shear Deformation Theory (FSDT) and Higher-Order Shear Deformation Theory (HSDT) were employed to account for shear effects. These latter theories were adopted because they consider shear deformation with high precision, unlike classical theories that neglect this important action. The equilibrium equations, derived from Hamilton's principle, were used, and Navier-type solutions were preferred to calculate buckling loads under uniaxial or biaxial loading. Parametric variations and different buckling modes were investigated, and the results showed excellent agreement with existing references. The main objective of this study in civil engineering is to continuously find mathematical formulations to solve plate buckling problems with extreme accuracy and to predict buckling behavior in simulations, mimicking what happens to metallic structures.

Keywords: Plate Buckling-Elastic Instability-Isotropic Metal Plate-First-Order Shear Deformation Theory (FSDT)-Higher-Order Shear Deformation Theory (HSDT).

النموذج الرياضي المقارب لدراسة سلوك انبعاج صفيحة فولاذية

عبد المطلب بن فريد، محمد بشير بويجرة

مخبر الهياكل والمواد المتقدمة في الهندسة المدنية والأشغال العمومية جامعة جيلالي اليابس سيدي بلعباس الجزائر
الجمهورية الجزائرية

الملخص:

تم إجراء دراسة رياضية للتحقق من التواء الألواح الفولاذية متساوية الخواص باستخدام نظريات عدم الاستقرار. تم استخدام نظرية تشوه القص من الدرجة الأولى (FSDT) ونظرية تشوه القص من الدرجة الأعلى (HSDT) لأخذ تأثيرات القص في الاعتبار تم اعتماد هذه الأخيرتين لأنهما تأخذا التشوه القصي بغاية العناية عكس النظريات الكلاسيكية التي تتجاهل هذا الفعل الهام. استخدمت معادلات التوازن المستمدة من مبدأ هاملتون، وتم تفضيل حلول نافبي لحساب أحمال التواء تحت أحمال أحادية أو ثنائية الاتجاه. تم التحقيق في التغييرات البارامترية وأنماط التواء مختلفة، وأظهرت النتائج توافقاً ممتازاً مع المراجع الموجودة. الهدف الرئيسي من هذه الدراسة في الهندسة المدنية هو محاولة إيجاد صيغ رياضية دوما لحل مشكل انبعاج الصفائح بدقة متناهية وكذا التنبأ المسبق للانبعاج محاكاتها لما يحدث لها في الهياكل المعدنية.

الكلمات المفتاحية: التواء الألواح - عدم الاستقرار المرن - ألواح معدنية متساوية الخواص - نظرية تشوه القص من الدرجة الأولى (FSDT) - نظرية تشوه القص من الدرجة الأعلى (HSDT).

1. Introduction

Steel construction, the second most common method after reinforced concrete, is gaining significant popularity due to its rapid execution and versatility. As countries around the world increasingly adopt steel construction techniques, there is a noticeable trend of national and private enterprises investing in this sector to stimulate economic growth. This shift can be attributed to the rise in global industrial and energy demands, which has led to a significant increase in the construction of steel structures such as factories, warehouses, and infrastructure projects. Steel construction involves the prefabrication and assembly of various components, which are scientifically referred to as beams, columns, and plates. The advantages of steel, including its high strength-to-weight ratio and durability, make it an ideal choice for modern construction practices. In this context, this study examines buckling instability in steel plates, which is a critical consideration in ensuring structural integrity and safety [1].

To address plate buckling effectively, appropriate theoretical frameworks are employed, including Classical Plate Theory (CPT), First-Order Shear Deformation Theory (FSDT), and Higher-Order Shear Deformation Theory (HSDT). These theories facilitate the

derivation of equilibrium equations that are essential for solving buckling problems and determining the critical buckling load. The study specifically analyzes isotropic and orthotropic rectangular plates using CPT as well as various HSDT models. By employing Navier's method to solve the governing equations, the research evaluates critical buckling loads (N_{cr}) across different plate thicknesses. A thorough discussion is provided on the methodologies for calculating the most accurate buckling loads, including the implications of material properties and geometric configurations on the buckling behavior of plates. The findings contribute valuable insights to the field of structural engineering, particularly in optimizing the design of steel structures to mitigate the risks associated with buckling instability [2].

In FSDT, a correction factor is used, which approximates, through a Taylor series, the ratio of 5/6. In contrast, in HSDT, different functions are employed to estimate the shear effect, often in the form of trigonometric or hyperbolic functions, among others. For this reason, in this work, we propose a new correction factor that depends on material parameters (such as Poisson's ratio). In both FSDT and HSDT, we derived a new function from the combinatorial combination of the two declared types of functions. The precision of the calculations is well demonstrated in the results, showing a perfect agreement with the expected outcomes. There are many steel structure regulations for estimating the local buckling of plates or panels, but they often use overly high correction factors. This leads to problems of underestimation or excessive construction costs. However, real studies that use mathematical analogies produce accurate results. Based on these results, we can ensure better calculation regulations through empirical formulas.

2. Mathematical model

Buckling is easily solved using elasticity theories known in material strength and matrix calculations in civil engineering structures.

The displacement field is expressed as follows:

$$\begin{cases} U(x, y, z) = u_0(x, y) + z \frac{\partial w_b}{\partial x} + z \cdot f(z) \cdot \frac{\partial w_s}{\partial x} \\ U(x, y, z) = v_0(x, y) + z \frac{\partial w_b}{\partial y} + z \cdot f(z) \cdot \frac{\partial w_s}{\partial y} \\ W(x, y, z) = w_a(x, y) + w_b(x, y) + w_s(x, y) \end{cases} \quad (1)$$

With: Angular rotation about the x or y axis.

$f(z)$ is the function used to estimate the shear deformation.

$$\left\{ \psi_x = \frac{\partial w_0}{\partial x} ; \psi_y = \frac{\partial w_0}{\partial y} \right. \quad (2)$$

The strain field is expressed according to the laws of elasticity as follows:

$$\begin{cases} \varepsilon_x = \frac{\partial U}{\partial x} \\ \varepsilon_y = \frac{\partial V}{\partial y} \\ 2\gamma_{xy} = \frac{\partial U}{\partial y} + \frac{\partial V}{\partial x} ; 2\gamma_{xz} = \frac{\partial U}{\partial z} + \frac{\partial W}{\partial x} \\ 2\gamma_{yz} = \frac{\partial V}{\partial z} + \frac{\partial W}{\partial y} \end{cases} \quad (3)$$

The stress tensor is:

$$[\sigma] = \begin{Bmatrix} \sigma_x \\ \sigma_y \\ \tau_{xy} \\ \tau_{xz} \\ \tau_{yz} \end{Bmatrix} = \begin{bmatrix} \bar{Q}_{11} & \bar{Q}_{12} & 0 & 0 & 0 \\ \bar{Q}_{12} & \bar{Q}_{22} & 0 & 0 & 0 \\ 0 & 0 & \bar{Q}_{66} & 0 & 0 \\ 0 & 0 & 0 & \bar{Q}_{55} & 0 \\ 0 & 0 & 0 & 0 & \bar{Q}_{44} \end{bmatrix} \begin{Bmatrix} \varepsilon_x \\ \varepsilon_y \\ 2\gamma_{xy} \\ 2\gamma_{xz} \\ 2\gamma_{yz} \end{Bmatrix} \quad (4)$$

Given that the material is isotropic, then:

$$\bar{Q}_{12} = \frac{E\theta}{(1-\theta^2)} ; \bar{Q}_{11} = \bar{Q}_{22} = \bar{Q}_{66} = \bar{Q}_{55} = \bar{Q}_{44} = \frac{E(1-\theta)}{2(1-\theta^2)} \quad (5)$$

Returning to Hamilton's principle:

$$\int_0^t (\delta U + \delta V) dt = 0 \quad (6)$$

Such that:

$$\delta U = \int (\sigma_{ij} \delta \varepsilon_{ij} + 2\tau_{ij} \delta \gamma_{ij}) dv \quad (7)$$

$$\delta V = \int \left(\frac{\sigma_{ijM}}{2} \delta \left(\frac{\partial W}{\partial x, y} \right)^2 + 2\tau_{ijM} \left(\frac{\partial W}{\partial x} \frac{\partial W}{\partial y} \right) \right) dv \quad (8)$$

Given that the resulting forces and moments are expressed in the form: :

$$\begin{cases} N_{ij} = \int_{-\frac{h}{2}}^{\frac{h}{2}} \sigma_{ij} dz \\ N_{ij}^M = \int_{-\frac{h}{2}}^{\frac{h}{2}} \sigma_{ijM} dz \\ M_{ij} = \int_{-\frac{h}{2}}^{\frac{h}{2}} \sigma_{ij} \cdot z dz \\ M_{ij}^M = \int_{-\frac{h}{2}}^{\frac{h}{2}} \sigma_{ijM} \cdot z dz \end{cases} \quad (9)$$

It is straightforward to obtain the equilibrium equations. The equilibrium equations are:

$$\left\{ \begin{array}{l} \delta u: \frac{\partial N_x}{\partial x} + \frac{\partial N_{xy}}{\partial y} = 0 \\ \delta v: \frac{\partial N_y}{\partial y} + \frac{\partial N_{xy}}{\partial x} = 0 \\ \delta w_b: \frac{\partial^2 M_x^b}{\partial x^2} + 2 \frac{\partial^2 M_{xy}^b}{\partial x \partial y} + \frac{\partial^2 M_y^b}{\partial y^2} + N^M(w) = 0 \\ \delta w_s: \frac{\partial^2 M_x^s}{\partial x^2} + 2 \frac{\partial^2 M_{xy}^s}{\partial x \partial y} + \frac{\partial^2 M_y^s}{\partial y^2} + \frac{\partial Q_{xz}^s}{\partial x} + \frac{\partial Q_{yz}^s}{\partial y} + N^M = 0 \\ \delta w_a: \frac{\partial Q_{xz}^a}{\partial x} + \frac{\partial Q_{yz}^a}{\partial y} + N^M(w) = 0 \end{array} \right. \quad (10)$$

En utilisant la technique de Navier, les solutions pour les plaques simplement appuyées sont obtenues

$$\left\{ \begin{array}{l} u(x, y) = U_m n \cos(tx) * \sin(py) \\ v(x, y) = V_m n \sin(tx) * \cos(py) \\ w_b(x, y) = W_b m n \sin(tx) * \sin(py) \\ w_s(x, y) = W_s m n \sin(tx) * \sin(py) \\ w_a(x, y) = W_a m n \sin(tx) * \sin(py) \end{array} \right. \quad (11)$$

Where:

$$t = \frac{m\pi}{a} \quad p = \frac{n\pi}{b} \quad (12)$$

(m,n) sont les modes de flambement .

The reduced stiffness matrix is written as:

$$\begin{bmatrix} K_{11} - N^0 N' & K_{12} & K_{13} \\ K_{12} & K_{22} & K_{23} \\ K_{13} & K_{23} & K_{33} \end{bmatrix} \begin{Bmatrix} W_{mn} \\ X_{mn} \\ Y_{mn} \end{Bmatrix} = \begin{Bmatrix} 0 \\ 0 \\ 0 \end{Bmatrix} \quad (13)$$

Calculate the determinant of this matrix in order to solve for the buckling load.

$$N^1 = \text{solve} [\text{DET}(K_{ij})] = 0 \quad (14)$$

When:

$$N^V = \alpha^2 + X * \beta^2 \quad (15)$$

The dimensionless critical load is given by the following relation:

$$N_{cr} = \frac{N^1 a^2}{Eh^3} \quad (16)$$

The parameters for the plate analysis include its length (a), width (b), and thickness (h). Notably, when (X=1), loading occurs in both directions, whereas when (X=0), loading is applied in only one direction.

3. Results and Discussion

Comparison of Models and Results:

To confirm the accuracy of our mathematical model, it is essential to compare it with existing models found in the literature. Table 1 presents the shear correction factors for the FSDT theory alongside three higher-order shear functions. The isotropic plate in question is characterized by the following mechanical properties: Young's modulus $E=200$ GPa. And Poisson's ratio $\nu=0.3$

The HSDT functions and shear correction factors for FSDT are:

KARAMA [3]

$$f(z) = z * e^{-2\left(\frac{z}{h}\right)^2} \quad (17)$$

AMBARTSUMIAN [4]

$$f(z) = \frac{z}{2} \left(\frac{h^2}{4} - \frac{z^2}{3} \right) \quad (18)$$

Touratier [5]

$$f(z) = \frac{h}{\pi} \sin\left(\frac{\pi z}{h}\right) \quad (19)$$

FSDT 1 [6]

$$K_s = 0.291 \quad (20)$$

FSDT 2 [7]

$$K_s = \frac{5}{6-\theta} \quad (21)$$

FSDT 3 [7]

$$K_s = \frac{5}{6-2\theta} \quad (22)$$

Present work :

For FSDT:

$$K_s = \frac{5}{6-\theta^4} \quad (23)$$

For HSDT:

$$f(z) = z - h * \arctang\left(\frac{z}{\pi * h}\right) + \frac{13}{19} * \left(\frac{z}{h}\right)^2 \quad (24)$$

Table 1. Comparison of the Critical Buckling Load N_{cr} for Biaxial Loading ($X=1$) of a Square Isotropic Steel Plate ($a=b$) as a Function of the Geometric Ratio (a/h) To compare the literature with the new work in order to validate our calculation model.

Previous Works	Mode	Theories	The geometric ratio ($\frac{a}{h}$).				
			5	10	20	50	100
	(1,1)	TSDT [8]	1.513	1.727	1.791	1.810	1.812
		REDDY(HSDT) [9]	1.475	1.711	1.782	1.803	1.806
		MINDLIN(FSDT) [6]	1.474	1.711	1.782	1.803	1.806
		CPT [10]	1.807	1.807	1.807	1.807	1.807
		FSDT	1.474	1.711	1.782	1.804	1.807
Present		HSDT	1.741	1.732	1.788	1.805	1.807

Table 2. Comparison of the Critical Buckling Load N_{cr} for a Square Isotropic Steel Plate ($a=b$) Under Unidirectional Loading ($X=0$), as a Function of the Geometric Ratio (a/h) To compare the literature with the new work in order to validate our calculation model.

Previous Works	Mode	Theories	The geometric ratio ($\frac{a}{h}$).				
			5	10	20	50	100
	(1,1)	TSDT [8]	3.026	3.454	3.582	3.621	3.625
		REDDY(HSDT) [9]	2.951	3.422	3.564	3.606	3.613
		MINDLIN(FSDT) [6]	2.949	3.422	3.564	3.607	3.613
		CPT [10]	3.615	3.6152	3.615	3.615	3.615
		FSDT	2.989	3.444	3.587	3.623	3.624
Present		HSDT	3.078	3.461	3.573	3.607	3.611

Table 3. Variation of the Critical Buckling Load N_{cr} for Uniaxial Loading ($X=1$) of a Square Isotropic Steel Plate with ($a=5h$) and ($a=b$) as a Function of the Buckling Mode (n)

Mode (m, n)	FSDT ($X=0$)	HSDT ($X=0$)	FSDT ($X=1$)	HSDT ($X=1$)
(1,1)	3.4999	3.078	1.492	1.519
(1,2)	14.454	15.777	2.893	3.143
(1,3)	42.439	48.623	4.265	4.843
(1,4)	89.401	106.763	5.201	6.256

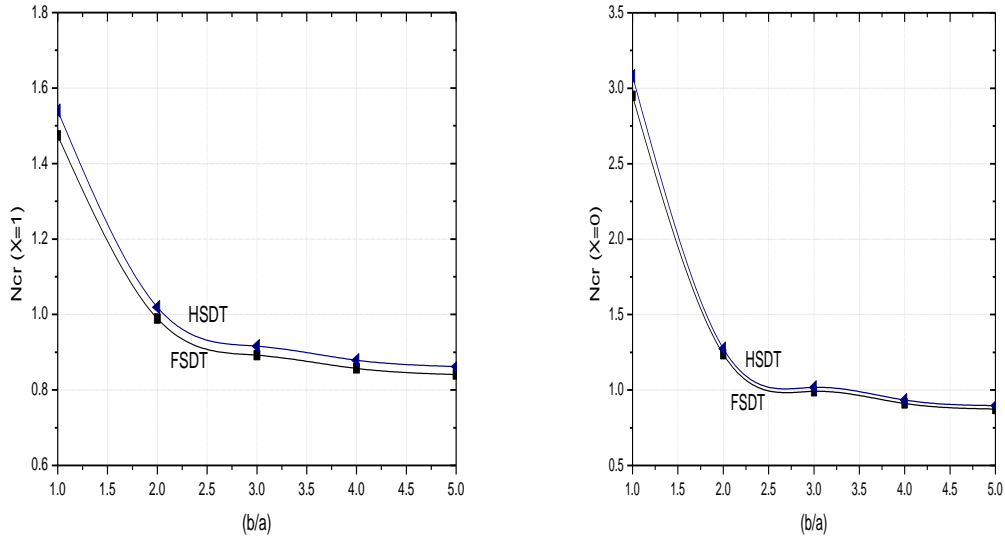


Figure 1. Variation of the Critical Buckling Load N_{cr} or Uniaxial Loading ($X=0$) and Biaxial Loading ($X=1$) of a Rectangular Isotropic Steel Plate with ($a=5h$) as a Function of the Geometric Ratio (b/a).

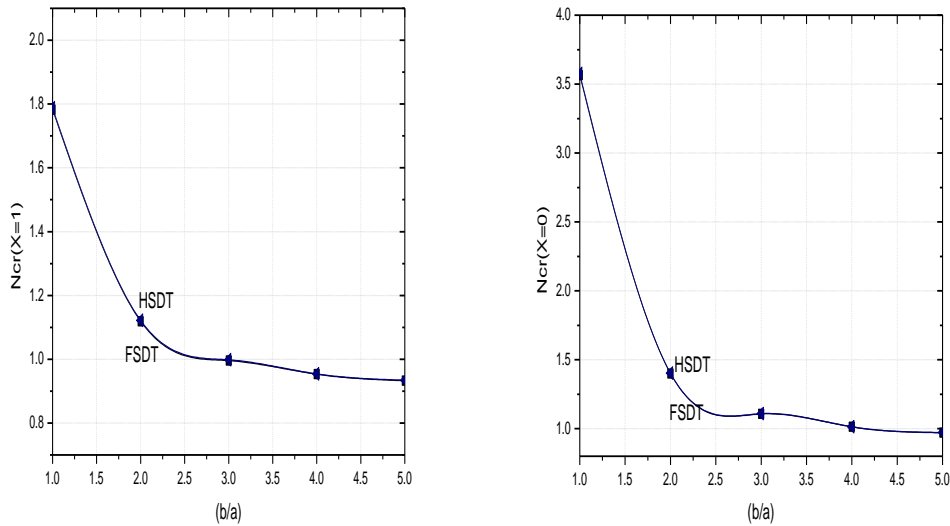


Figure 2. Variation of the Critical Buckling Load N_{cr} or Uniaxial Loading ($X=0$) and Biaxial Loading ($X=1$) of a Rectangular Isotropic Steel Plate with ($a=20h$) as a Function of the Geometric Ratio (b/a).

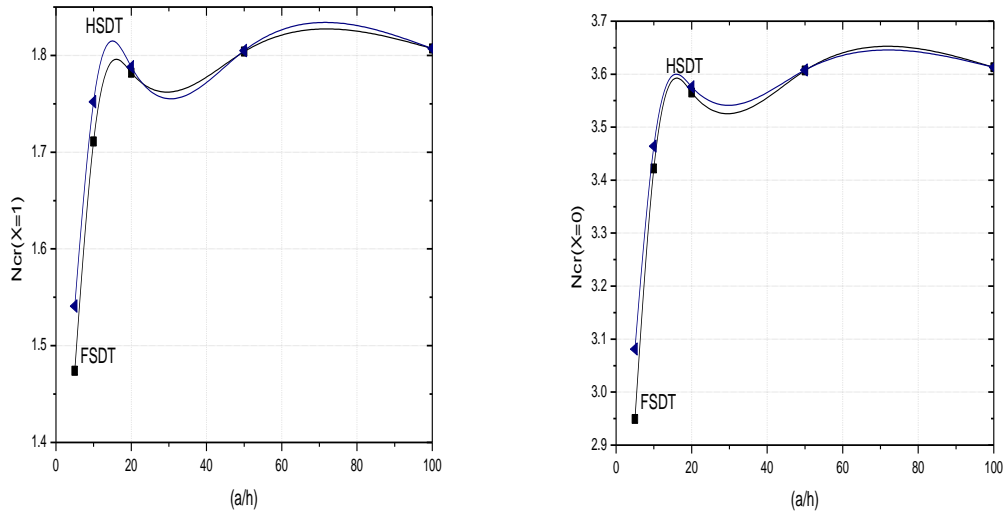


Figure 3. Variation of the Critical Buckling Load N_{cr} or Uniaxial Loading ($X=0$) and Biaxial Loading ($X=1$) of a Rectangular Isotropic Steel Plate with ($a=b$) as a Function of the Geometric Ratio (a/h).

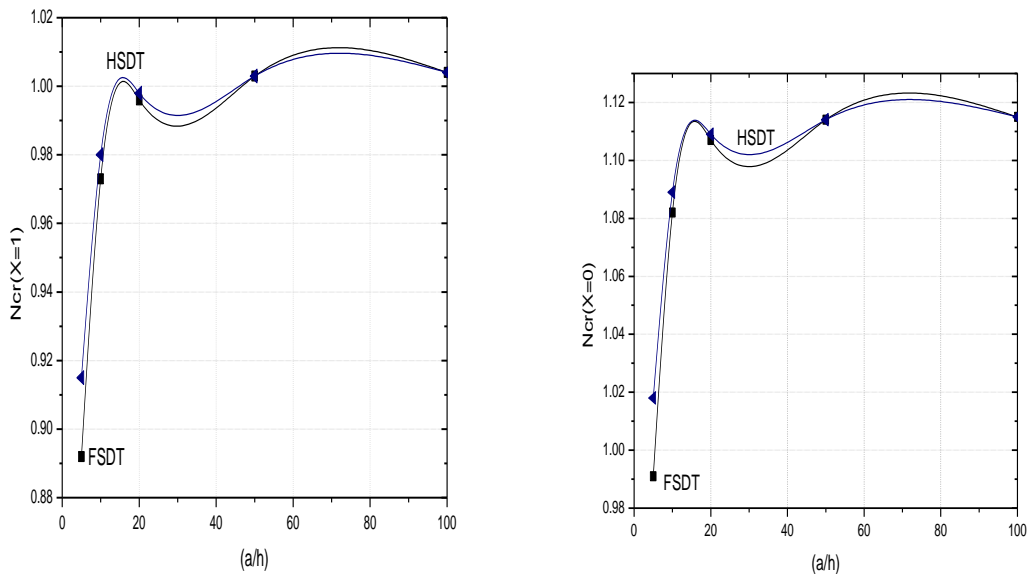


Figure 4. Variation of the Critical Buckling Load N_{cr} or Uniaxial Loading ($X=0$) and Biaxial Loading ($X=1$) of a Rectangular Isotropic Steel Plate with ($b=5a$) as a Function of the Geometric Ratio (a/h).

4. Results and Discussions:

The analysis presented in Table 1 demonstrates that our mathematical model has been validated by aligning closely with findings from existing literature. This validation is particularly evident when examining the behavior of square plates, where the dimensions are equal ($a = b$). In such cases, the critical buckling load is observed to increase as the ratio of the plate's side length (a) to its thickness (h) also increases. This relationship holds true across different functions utilized within Classical Plate Theory (CPT), specifically for a scenario where the dimension of the plate is significantly larger than its thickness, represented by the condition $a = 100h$.

Furthermore, when comparing different theoretical approaches, the First-Order Shear Deformation Theory (FSDT) yields results that are closely aligned with those derived from Higher-Order Shear Deformation Theory (HSDT), especially when the correction coefficient K_s approximates $5/6$. However, notable discrepancies arise within the HSDT results when the aspect ratio is set to $a = 5h$, indicating that the choice of theory can have significant implications on the outcomes, particularly in this range.

The analysis also reveals that the critical buckling load for a square plate subjected to uniaxial loading is significantly greater—approximately double—that of a plate experiencing biaxial loading conditions. This difference emphasizes the importance of loading conditions on buckling behavior and critical load determination. Additionally, it is observed that as the buckling modes vary, the critical load continues to increase; however, differences among the theoretical predictions become evident, as summarized in Table 3.

In the case of rectangular plates, the behavior is slightly different. The critical load decreases as the ratio of width to length (b/a) increases, stabilizing once this ratio reaches approximately 4. At lower values of the (a/h) ratio, the discrepancies between various theoretical predictions become more pronounced; however, as this ratio increases, the results from different theories converge. For both square and rectangular plates, the critical load N_{cr} consistently rises with increasing ratios of (a/h), reaching a stabilization point around a value of 45. Initially, there is considerable variation among different theories; however, as the analysis progresses, these differences diminish, indicating a convergence of results.

Another critical aspect of this study is the improvement in the shear deformation function $f(z)$, which plays a vital role, particularly in thin plates. This enhancement is visually represented in Figures 3 and 4, highlighting its impact on buckling behavior. The results obtained from this analysis not only contribute to our understanding of buckling phenomena but also serve to validate whether existing regulations and guidelines are applicable in practical scenarios.

Moreover, in situations where calculation methods or technical regulations are lacking, engineers must remain proactive. They cannot halt their work; instead, they must seek alternative solutions to accurately calculate buckling and critical buckling loads. This includes applying a slight amplification to the critical load N_{cr} in order to estimate the

dimensions of metallic panels or plates. This is particularly relevant in simpler structures, such as hydraulic and oil stations, where efficient design is crucial.

For instance, when considering thick plates, the first mode of buckling is often sufficient for analysis. In these cases, the results tend to be consistent, allowing engineers to focus on determining the critical N_{cr} alongside the ratios a/b and a/h , where a and b denote the dimensions of the plate and h represents its thickness. This approach streamlines the design process and ensures that structural integrity is maintained throughout various loading conditions.

5. Conclusion:

This work reveals several key findings:

- 1- Impact of Geometric Parameters: The geometric parameters of a plate—specifically its length, width, and thickness—play a crucial role in determining its critical buckling load. These parameters directly influence the load-bearing capacity of the plate, underscoring the importance of careful consideration during the design process.
- 2- Validity of Plate Theories: All evaluated plate theories demonstrate validity, albeit with some degree of uncertainty. This variability emphasizes the necessity of selecting the most appropriate model for specific applications. A careful choice of theory can significantly enhance the accuracy of predictions regarding buckling behavior, ultimately leading to safer and more effective engineering solutions.
- 3- Importance of Shear Deformation Functions: Within the framework of Higher-Order Shear Deformation Theory (HSDT), the selection of shear deformation functions is critical. These functions are essential for accurately capturing shear effects in isotropic plates, which in turn has a significant impact on the overall accuracy of the model. This highlights the need for further exploration and validation of different shear functions to optimize buckling analyses.
- 4- Correction Coefficient in FSDT: For the First-Order Shear Deformation Theory (FSDT), it has been observed that using a correction coefficient of approximately $5/6$ yields results that closely align with those obtained from HSDT. This adjustment effectively accounts for shear effects, thereby enhancing the reliability of the FSDT in practical applications.
- 5- Feasibility of Buckling Analysis: The buckling analysis of isotropic steel plates using various plate theories is not only feasible but also provides reliable methodologies for predicting buckling loads. These predictions are essential for design and safety assessments in a wide range of engineering applications, including civil and structural engineering.
- 6- Regulatory Implications: This study contributes to the verification and creation of technical regulations within the field of structural design. The findings can inform the development of new guidelines, ensuring that they reflect the latest advancements in plate buckling theory and practice.

References

- [1] C. TRUESDELL. " MECHANICS OF SOLIDS VOLUME II Linear Theories of Elasticity and Thermoelasticity Linear and Nonlinear Theories of Rods, Plates, and Shells" Springer-Verlag Berlin Heidelberg GmbH 1984, DOI 10.1007/978-3-662-39776-3
- [2] Bera, Puspendu, et al. "Buckling Analysis of Isotropic and Orthotropic Square/Rectangular Plates Using CLPT and Different HSDT Models." Materials Today: Proceedings 56, no. 1 (2022): 237-244.
- [3] Karama, M., K. S. Afaq, and S. Mistou. "Mechanical Behaviour of Laminated Composite Beam by the New Multi-Layered Laminated Composite Structures Model with Transverse Shear Stress Continuity." International Journal of Solids and Structures. Accessed August 6, 2024.
- [4] Ambartsumian, S. A. "On Theory of Bending Plates." Izvestiya Akademii Nauk SSSR, Otdelenie Tekhnicheskikh Nauk 5 (1958): 69–77.
- [5] [5] Touratier, M. "An Efficient Standard Plate Theory." Journal of Mechanics 91 (1991): 453-462.
- [6] Mindlin, R. D. "Influence of Rotatory Inertia and Shear on Flexural Motions of Isotropic, Elastic Plates." ASME Journal of Applied Mechanics 18 (1951): 31-38.
- [7] Efraim, E., and M. Eisenberger. "Exact Vibration Analysis of Variable Thickness Thick Annular Isotropic and FGM Plates." Journal of Sound and Vibration 299 (2007): 720-738.
- [8] Sayyad, A. S., and Y. M. Ghugal. "On the Buckling of Isotropic, Transversely Isotropic and Laminated Composite Rectangular Plates." International Journal of Structural Stability and Dynamics 14, no. 7 (2014): 1-32.
- [9] Bedilu Habte. " Matrix Structural Analysis and the Finite Element Methods Using Scilab and Octave A Problem-Solving Approach" First edition published 2025 by CRC Press 2385 NW Executive Center Drive, Suite 320, Boca Raton FL 33431. DOI: 10.1201/9781003329350
- [10] Kirchhoff, G. R. "Über das Gleichgewicht und die Bewegung einer elastischen Scheibe." Journal für die Reine und Angewandte Mathematik 40 (1850): 51-88.